Applied Mathematical Modelling 74 (2019) 606–620

Contents lists available at ScienceDirect

Applied Mathematical Modelling

journal homepage: www.elsevier.com/locate/apm

A dynamic multi-objective optimization model with interactivity and uncertainty for real-time reservoir flood control operation

Xiaolin Liu, Jungang Luo*

State Key Laboratory of Eco-hydraulics in Northwest Arid Region, Xi'an University of Technology, Xi'an 710048, China

ARTICLE INFO

Article history:
Received 30 July 2018
Revised 18 April 2019
Accepted 8 May 2019
Available online 16 May 2019

Keywords:
Reservoir flood control operation
Dynamic multi-objective optimization model
Interactivity
Evolutionary multi-objective optimization algorithm

ABSTRACT

Despite the successes of both multi-objective optimization and uncertainty handling techniques in reservoir flood control operation, no work has been done yet on developing and investigating dynamic multi-objective optimization models for this problem. In this work, a dynamic multi-objective optimization model with interactivity and uncertainty was developed for the real-time reservoir flood control operation. Accordingly, a dynamic multi-objective optimization algorithmic framework with two newly designed change reaction strategies was proposed for solving the proposed dynamic model. Following the proposed algorithmic framework, any evolutionary multi-objective optimization algorithm can be converted into a dynamic optimizer. After investigating the difficulty variation of the proposed dynamic model, the effectiveness and robustness of the proposed algorithmic framework have been validated based on experiential studies on two typical floods of Ankang reservoir.

1. Introduction

Reservoir flood control (RFC) operation is a challenging optimization problem that involves conflicting objectives on flood peak reduction, flood damage prevention, flood reservation and so on [1]. For a long time, the RFC problem was generally modeled as a single-objective optimization problem by optimizing the most important objective while considering some less important ones as constraints [2], or by aggregating some of the conflicting objectives into a comprehensive one [3]. However, with the significant progress of multi-objective optimization techniques in recent years, more and more research efforts have been focusing on handling the multi-objective RFC problem directly.

At present, many multi-objective reservoir flood control operation methods have been proposed, most of which were developed based on modern meta-heuristic optimization techniques [4,5]. These meta-heuristic optimizers can provide the decision maker with a various set of best trade-off scheduling plans, termed as Pareto optimal solutions. Despite the success of the multi-objective reservoir flood control operation algorithms, they have the same drawback of ignoring the uncertainty of the arriving floods [6]. Based on the hypothesis that each incoming flood might develop as the design flood, the optimized flood control rule curves are usually derived from the total hydrographs of project design floods.

To deal with the uncertainty of the floods and provide the decision maker with dynamic discharge rules, some real-time RFC algorithms have been developed, most of which combine the flood forecasting model with the deterministic

* Corresponding author.
E-mail addresses: lxl_xiaolin@163.com (X. Liu), jgluo@xaut.edu.cn (J. Luo).

https://doi.org/10.1016/j.apm.2019.05.009
0307-904X/

optimization model [6]. Some others apply different operation rules dynamically under various inflow alteration scenarios [7] or in different phases of a certain flood [8]. Although the above mentioned real-time RFC methods considered the uncertainty of the arriving floods, the optimization models for reservoir discharge rules were still static ones. In addition, there was no interaction with the decision maker during the optimization procedure.

In this work, a dynamic multi-objective optimization model with interactivity and uncertainty is proposed for the RFC problem. Accordingly, an algorithmic framework of real-time multi-objective optimizer, termed as the dynamic multi-objective RFC algorithm (DMO-RFC), is developed for solving the proposed model. Different from static multi-objective optimization models for RFC problems, the dynamic model divides the sequence of the reservoir inflow into two parts, the observed inflow sequence which has arrived at current scheduling time period and the forecasted inflow sequence which can be provided by a flood forecasting model. At each scheduling time period, the decision maker is requested to make a decision on the reservoir discharge volume by choosing a discharge water volume from a candidate set of Pareto optimal solutions provided by the DMO-RFC algorithm. After a sequence of decision-making, the number of decision variables of the dynamic model decreases with time, which is significantly different from the static models. To the best of our knowledge, this is the first work on modeling the RFC problem as a dynamic multi-objective optimization problem.

Since many optimization problems in practice involve multiple conflicting objectives and change over time in dynamic environments, dynamic multi-objective optimization techniques have received growing research interests in recent years [9]. The time-varying characteristics of optimization problems raise big challenges to evolutionary multi-objective optimizers which are demanded to be capable of tracking the changing of the problems and providing a diverse set of Pareto optimal solutions over time. At present, research works on developing dynamic multi-objective optimization algorithms mainly focused on the following four topics: 1) How to detect the changes of the problem [10]. 2) How to cope with the change and obtain satisfactory Pareto optimal solutions for the new problem [11]. 3) How to evaluate the performance of a dynamic multi-objective optimization algorithm [12]. 4) Applications on real-world problems [13]. Among existing works, the investigated dynamic multi-objective optimization models could have time-varying Pareto-optimal fronts, variable linkages or constraints, but all of them were supposed to have a determined number of decision variables. Therefore, existing dynamic multi-objective optimization algorithms can not be directly applied to the dynamic multi-objective RFC problem in which the number of decision variables decreases with time.

To remedy this, two change reaction strategies are developed to perform some actions in response to the changes of the dynamic multi-objective RFC model. One is the diversity maintaining strategy which re-initializes the evolving population after the change of environment by inheriting some of the Pareto optimal solutions for the previous problems and generating new solutions at random. The other is differential evolution (DE) based operator which performs local search in the decision space and has been proved to be efficient for multi-objective RFC problems [14]. These two strategies can be combined with any evolutionary multi-objective optimization algorithm to form a dynamic multi-objective RFC algorithm.

The main contributions of this paper can be summarized as follows:

1. A dynamic multi-objective optimization model with interactivity and uncertainty has been proposed for the RFC problem.
2. By investigating the Pareto-optimal fronts of the proposed dynamic multi-objective optimization model at a sequence of scheduling time periods, the changing of the complexity of each instantaneous multi-objective optimization problem has been revealed.
3. Two change reaction strategies have been developed to perform some actions in response to the changes of the dynamic multi-objective RFC model.
4. By combining the proposed change reaction strategies with any evolutionary multi-objective optimization algorithm, a dynamic multi-objective algorithmic framework for RFC problem (DMO-RFC) has been proposed.

The remainder of this paper is organized as follows. Section 2 describes the proposed dynamic multi-objective optimization model for RFC problem. Section 3 describes the idea and the implementation of the proposed DMO-RFC algorithm for solving the dynamic multi-objective RFC problem. Section 4 reports and analyzes the experimental results. Section 5 concludes this paper.

2. The dynamic multi-objective optimization model for RFC problem

During floods, the safety of both upstream and downstream of the dam becomes the most important issue. To guarantee the safety of the upstream side, the upstream water level must not be too high. However, this will threaten the safety of downstream side seriously when encountering a big flood. The safety of the downstream side requires that the water discharge flow cannot be too large.

Suppose the arriving flood lasts for T scheduling time periods. At each scheduling time period of t $(t = 1, 2, \ldots, T)$, the reservoir discharge flow $\mathbf{Q}^t = (\bar{Q}_1^t, \bar{Q}_2^t, \ldots, \bar{Q}_{t-1}^t, Q_t^t, Q_{t+1}^t, \ldots, Q_T^t)$ which is the decision vector of the tth instantaneous multi-objective optimization problem can be divided into two parts. The immutable part $\{\bar{Q}_1^t, \bar{Q}_2^t, \ldots, \bar{Q}_{t-1}^t\}$, which has been determined by the decision maker in previous interactions, and the mutable part $\{Q_t^t, Q_{t+1}^t, \ldots, Q_T^t\}$ needs to be optimized. At the same time, the reservoir inflow at the tth scheduling time period $\mathbf{I}^t = (\bar{I}_1^t, \bar{I}_2^t, \ldots, \bar{I}_{t-1}^t, I_t^t, I_{t+1}^t, \ldots, I_T^t)$ is also formed by two parts, the observed part $\{\bar{I}_1^t, \bar{I}_2^t, \ldots, \bar{I}_{t-1}^t\}$ and the forecasted part $\{I_t^t, I_{t+1}^t, \ldots, I_T^t\}$.

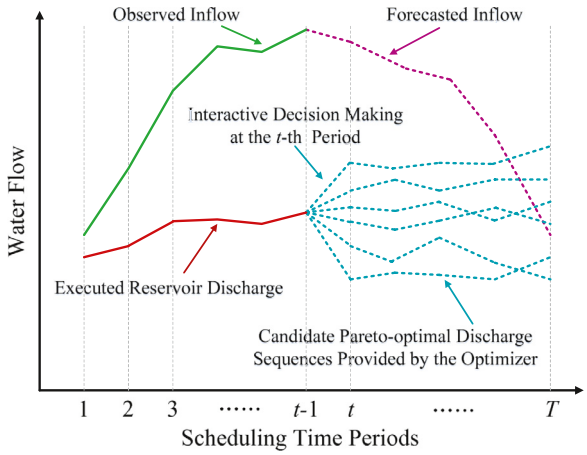

Fig. 1. The sequential interactive decision-making process based on the dynamic multi-objective optimization model for RFC problem.

Analogously, denote $\mathbf{Z}^t = (\bar{Z}_1^t, \bar{Z}_2^t, \ldots, \bar{Z}_{t-1}^t, Z_t^t, Z_{t+1}^t, \ldots, Z_T^t)$ as the sequence of the dam's upstream water levels at the tth scheduling time period and $\mathbf{V}^t = (\bar{V}_1^t, \bar{V}_2^t, \ldots, \bar{V}_{t-1}^t, V_t^t, V_{t+1}^t, \ldots, V_T^t)$ as the sequence of reservoir storages. Considering the safety of both upstream and downstream of the reservoir during floods, a dynamic multi-objective optimization model, which can be mathematically formulated as Eq. (1), is proposed for RFC Problem.

$$
\begin{aligned}
&\text{Minimize} \quad \mathbf{F}(\mathbf{Q^t}, \mathbf{I^t}) = (f_1(\mathbf{Q}^t, \mathbf{I}^t), f_2(\mathbf{Q}^t, \mathbf{I}^t)) \\
&\quad f_1(\mathbf{Q}^t, \mathbf{I}^t) = \max\{\mathbf{Z}^t\} \\
&\quad f_2(\mathbf{Q}^t, \mathbf{I}^t) = \max\{\mathbf{Q}^t\} \\
&\text{Subject to} \\
&\quad Z_{min} \le Z_i^t \le Z_{max}, \quad i = t, \ldots, T \\
&\quad 0 \le Q_i^t \le Q_{max}, \quad i = t, \ldots, T \\
&\quad V_i^t = V_{i-1}^t + I_i^t - Q_i^t, \quad i = t, \ldots, T \\
&\quad t = 1, 2, \ldots, T
\end{aligned}
\tag{1}
$$

The objective vector $\mathbf{F}(\mathbf{Q^t}, \mathbf{I^t})$ has two components, i.e. $f_1(\mathbf{Q}^t, \mathbf{I}^t)$ and $f_2(\mathbf{Q}^t, \mathbf{I}^t)$. The first optimization objective $f_1(\mathbf{Q}^t, \mathbf{I}^t)$ is to minimize the highest upstream water level, with the aim of ensuring the safety of the dam and decrease loss of upstream area. The second optimization objective $f_2(\mathbf{Q}^t, \mathbf{I}^t)$ is to minimize the largest discharge volume, and to protect the downstream areas. There are three constraints in the proposed model. The constraint (1) guarantees that the upstream water level Z_i^t lies between the lower bound of Z_{min} and the upper bound of Z_{max}. The constraint (2) defines the boundary of the reservoir discharge volume Q_i^t at each scheduling time period. The constraint (3) is the water balance condition. In multi-objective optimization problems, no unique solution could meet all the conflicting objectives. Instead, there exists some best trade-offs which are known as Pareto-optimal solutions. The collection of all the Pareto optimal solutions in the decision space is termed as the Pareto set (PS) whose image in the objective space is called the Pareto front. The aim of a multi-objective optimization algorithm is to obtain a finite set of representative solutions with good approximation, coverage and uniformity over the Pareto front of the target problem.

With the proposed dynamic multi-objective optimization model for RFC problem, the decision maker can interact with the optimizer at each scheduling time period and determine an appropriate reservoir discharge volume from a candidate set of Pareto optimal solutions provided by the multi-objective optimization algorithm for each instantaneous problem. The sequential interactive decision-making process based on the dynamic multi-objective optimization model for RFC problem is illustrated by Fig. 1.

As shown in Fig. 1, the instantaneous multi-objective RFC problem at the tth scheduling time period takes the forecasted inflow as input, and determines current upstream water level based on the observed inflow and the executed reservoir discharge. The dynamic multi-objective optimizer provides the decision maker with a set of candidate Pareto-optimal discharge sequences. Then, the decision maker is required to determine the discharge volume to be executed at the tth scheduling time period. With this interactive decision-making, the sequence of the executed reservoir discharge increases with time, and the whole discharge curve can be generated at the end of the flood. It can be seen that as time goes on, the number of decision variables of the dynamic model decreases from T to 1.

3. DMO-RFC: the proposed algorithmic framework

Adapting search behavior quickly to the environmental changes is a key issue in dealing with dynamic multi-objective optimization problems. For this reason, change detection and change reaction are the two major components of dynamic

multi-objective optimization algorithms. Since the environment always changes in the RFC problem, the dynamic multi-objective RFC problem changes at every single scheduling time period. Therefore, the change reaction strategy plays the most importance role in the dynamic multi-objective RFC algorithm.

In this work, two change reaction strategies have been developed to perform actions in response to the changes of the dynamic multi-objective RFC model. One is the diversity maintaining strategy implemented by the "Re-Initialization" step in the following Algorithm 1. The other is the differential evolution (DE) based operator which performs local search in the

Algorithm 1 DMO-RFC: a dynamic multi-objective algorithmic framework for RFC problem.

Input: $\mathbf{F}(\mathbf{Q^t}, \mathbf{I^t})$: The dynamic multi-objective RFC problem, MOEA: A multi-objective evolutionary algorithm, T: The total scheduling time periods.
Output: $\mathbf{Q}^T$: The sequence of reservoir discharge volumes.
1: $InitPOP^1 \leftarrow$ **Random-Initialization**();
2: $POP^1 \leftarrow$ **MOEA-DE**($InitPOP^1$);
3: $Q_1^1 \leftarrow$ **Interactive-Decision-Making**(POP^1)
4: **for** t= 2 to T **do**
5: $InitPOP^t \leftarrow$ **Re-Initialization**(POP^{t-1}, Q_t^{t-1});
6: $POP^t \leftarrow$ **MOEA-DE**($InitPOP^t$);
7: $Q_t^t \leftarrow$ **Interactive-Decision-Making**(POP^t)
8: **end for**
9: Return $\mathbf{Q}^T$

employed multi-objective evolutionary algorithm and implemented by the "DE-Operator". By combining these two change reaction strategies with any evolutionary multi-objective optimization algorithm, the proposed algorithmic framework of dynamic multi-objective RFC algorithm works as the following Algorithm 1.

In Algorithm 1, the population is randomly initialized (in line 1) with the aim of maintaining a good initial population diversity. Then, the initial population is evolved by the employed population evolving algorithm MOEA-DE (in line 2) at the beginning of the flood. In line 3, the decision maker is required to determine reservoir discharge volume at the first scheduling time period. For the next instantaneous problem, the initial population is generated by the diversity maintaining strategy, which is implemented by the "Re-Initialization" operation in line 5 and described in detail in Algorithm 2. The

Algorithm 2 Re-Initialization(POP^t, Q_t^t).

Input: POP^t: The evolved population for the tth instantaneous problem, N: the population size, Q_t^t: The reservoir discharge volume at the tth scheduling time period.
Output: $InitPOP^{t+1}$: The initial population for the next instantaneous problem.
1: $\mathbf{I} \leftarrow$ Select $0.1 * N$ individuals from POP^t at random;
2: Replace the value of the tth dimension of each individual in $\mathbf{I}$ with Q_t^t;
3: $\mathbf{R} \leftarrow$ Generate $0.9 * N$ individuals at random;
4: Replace the values of the 1st to tth dimension of all the individuals in $\mathbf{R}$ with $(\bar{Q}_1^t, \bar{Q}_2^t, \ldots, \bar{Q}_t^t)$ which is progressively determined by the decision maker in the 1st to the tth scheduling time periods.
5: $InitPOP^{t+1} = \mathbf{I} \cup \mathbf{R}$.
6: Return $InitPOP^{t+1}$

initial population is then evolved by MOEA-DE in line 6, giving rise to a set of candidate solutions POP^t. In line 7, an interactive decision-making process is performed by the decision maker, and the reservoir discharge volume at the tth scheduling time period is determined. After iterations, the sequence of reservoir discharge volumes $\mathbf{Q}^T$, as the output of the algorithm, can be progressively determined.

Given the evolved population for previous instantaneous problem POP^t $(t = 1, 2, \ldots T)$ with N individuals and the reservoir discharge volume Q_t^t at the tth scheduling time period determined by the decision maker, the "Re-Initialization" operation works as the following Algorithm 2.

In Algorithm 2, the initial population for the next instantaneous problem is composed of two parts, i.e. the union of the individual set of $\mathbf{I}$ and the individual set of $\mathbf{R}$ (in line 5). 10% individuals are inherited from the previous population ($\mathbf{I}$, in lines 1 and 2) and 90% individuals are newly generated at random($\mathbf{R}$, in lines 3 and 4). As we know, the ratios of population inheriting and diversity promoting depend on the change of the target problem, an efficient dynamic multi-objective evolutionary algorithm should make a good balance between them. Based on our observations, when the population inheriting ratio has a value between 5% and 15%, the proposed algorithm can obtain satisfactory performances on all the investigated study cases at most scheduling time periods. To avoid too many parameters, we set the ratios of population inheriting and diversity promoting to 10% and 90% respectively.

In the re-initialized population, the first t dimensions of each individual have been determined by the decision maker at previous interactions, while the rest dimensions are mutable and need to be optimized. With this diversity maintaining

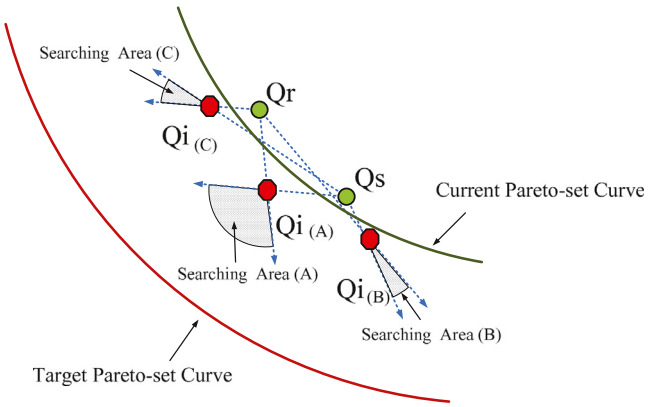

Fig. 2. The design principle of the DE-Operator.

strategy in Algorithm 2, some the Pareto-optimal solutions for the previous instantaneous problem can be inherited by the initial population for the consequential problem to accelerate the evolving process of the DMO-RFC algorithm. Meanwhile, some new individuals with greater diversity are generated at random to enhance the adaptability of the DMO-RFC algorithm to environmental changes.

Algorithm 3 DE-Operator(*POP*).

Input: *POP*: The evolving population with N individuals.
Output: *POP*′: The newly generated population.
1: Let *POP*′ be an empty set.
2: **for** each individual **Qi** $(i = 1, 2, \ldots, N)$ in *POP* **do**
3: Select **Qr** and **Qs** $(r, s = 1, 2, \ldots, N)$ at random from *POP*;
4: Generate a new individual **Q**′ based on **Qi**, **Qr** and **Qs** as follows:

$$\mathbf{Q}' = \mathbf{Qi} + rand(0,1) * (\mathbf{Qr} - \mathbf{Qi}) + rand(0,1) * (\mathbf{Qs} - \mathbf{Qi}) \tag{2}$$

5: $POP' = POP' \cup \{\mathbf{Q}'\}$;
6: **end for**
7: Output *POP*′;

The other change reaction strategy is the differential evolution based operator (DE-Operator), as described in Algorithm 3. Given an evolving population with N individuals, the DE-Operator generates one offspring for each individual, giving rise to a newly generated population with the same size.

According to Eq. (2), the DE-Operator generates a new offspring based on three parent individuals. Given a parent individual **Qi** and another two individuals **Qr** and **Qs**, the DE-Operator performs a local search nearby **Qi** along the direction determined by $\mathbf{Qr} - \mathbf{Qi}$ and $\mathbf{Qs} - \mathbf{Qi}$. The design principle of the DE-Operator is illustrated by Fig. 2.

As shown in Fig. 2, individuals **Qr, Qs** and **Qi** within current evolving population locate nearby the current Pareto-set curve in the decision space. **Qi** can locate between **Qr** and **Qs** (denoted as **Qi**(A)) or beside the two points (denoted as **Qi**(B) and **Qi**(C)). According to Eq. (2), the DE-Operator is expected to provide search directions with two types. For the scenario of **Qi**(A), the DE-Operator performs an exploitation local search between **Qr** and **Qs** towards the target Pareto-set curve. As for the scenarios of **Qi**(B) and **Qi**(C), the DE-Operator performs an exploration search toward even wider areas to generate more diversity.

By combing with the above described DE-Operator, any multi-objective evolutionary algorithm (MOEA) that follows the general framework of Algorithm 4, such as the NSGA-II [15] and the MOEA/D [16] algorithm, can be converted into its variant version denoted as **MOEA-DE**(*InitPOP*). The latter is then employed as population evolving steps in Algorithm 1 (line 2 and line 6) to form a dynamic optimizer for solving the dynamic multi-objective optimization model for RFC, as defined by Eq. (1).

In fact, Algorithm 4 is a brief description of all the MOEAs in literature, which evolves a population of individuals via reproduction, including crossover (line 3) and mutation (line 4) steps, and selection (line 5) iterations.

The *MOEA-DE*(*InitPOP*) follows all the main steps of Algorithm 4, but replaces the crossover step in line 3 with the DE-Operator described in Algorithm 3. It starts from an initial population of individuals and reproduces new offspring by using the DE-Operator (Algorithm 3) and mutation (the same as used in the original MOEA) operators. After the reproduction steps, a selection procedure is then performed to choose a determined number of individuals with high quality from the joint set of the old and the new population, giving rise to the improved population for the next iteration. Such reproduction

Algorithm 4 **MOEA**(*InitPOP*).

Input: *InitPOP*: The initial population;
Output: *POP*: The evolved population.
1: **Initialization**: $POP \leftarrow InitPOP$;
2: **while** If stopping condition is not met **do**
3: **Crossover**: $POP' \leftarrow Corssover(POP)$;
4: **Mutation**: $POP'' \leftarrow Mutation(POP')$;
5: **Selection**: $POP \leftarrow POP \cup POP''$
6: **end while**
7: Output *POP*;

and selection procedures repeat until the stopping condition is met. With the evolving of the population, the quality of the individuals will be improved gradually and the problems will be solved after iterations.

When considering the computational complexity of the proposed DMO-RFC algorithm (in Algorithm 1), the *Random-Initialization* step in line 1 and the *Re-Initialization* step in line 5 take a computational complexity of $O(N)$ in which N is the population size. The *Interactive-Decision-Making* steps in lines 3 and 7 are performed by the decision maker who is required to investigate the N evolved individuals provided by the optimizer of *MOEA-DE* and make a decision on the reservoir discharge volume at each scheduling time period. Therefore, the *Interactive-Decision-Making* step has a computational complexity of $O(N)$. As for the population evolving steps, say *MOEA-DE*, in lines 2 and 6, both the *DE-Operator* and the *Mutation* step have a computational complexity of $O(N)$. The computational complexity of the *Selection* step depends on the employed MOEA instance. For example, when the NSGA-II algorithm which is a non-dominated sorting based MOEA is employed as the population evolving algorithm, the *Selection* step has a computational complexity of $O(MN^2)$ in which M is the number of objectives [15]. When the MOEA/D algorithm which is a decomposition based MOEA is employed, the *Selection* step will take a computational complexity of $O(MN^SN)$ in which M is the number of objectives and N^S is the size of the neighborhood list of each decomposition weight [16]. If the *MOEA-DE* algorithm is allowed to evolve g generations, then the computational complexity of the *MOEA-DE* step is $O(gMN^2)$ for NSGA-II implementation and $O(gMN^SN)$ for MOEA/D implementation. Therefore, the overall computational complexity of DMO-RFC algorithm is $O(T(N+N+gMN^2))$, say $O(TgMN^2)$, for NSGA-II implementation and $O(T(N+N+gMN^SN))$, say $O(TgMN^SN)$, for MOEA/D implementation, in which T is the total number of scheduling time periods.

4. Experimental studies

In this section, the investigated floods and employed performance metric will be introduced at first. Then, by investigating the changes of the Pareto fronts of instantaneous multi-objective RFC problems at a sequence of scheduling time periods, a theoretical analysis on the proposed dynamic multi-objective optimization model for RFC problem will be made. After that, the superiority of the proposed DMO-RFC framework will be validated by investigating its two implementations combined with the NSGA-II [15] and the MOEA/D [16] algorithms which are two of the most popular multi-objective optimization algorithms. Finally, the robustness of DMO-RFC to the reservoir forecasting error will be analyzed.

4.1. The study cases

The Ankang reservoir on the Hanjiang river is a large reservoir with the purpose of flood control, power generation, water supply, and so on. The Ankang reservoir was first built in October 1982 with an area of 77.5 km^2, and maximum water capacity of 2.585 billion m^3. It has a normal water level of 330 m, a flood control limit level of 325 m and a dead water level of 300 m. The designed discharge capacity of the Ankang reservoir is 37,474 m^3/s. Two typical floods of the Ankang reservoir were used as study cases in the experimental studies.

Fig. 3 illustrates the reservoir inflow of the two investigated floods. The flood on August 28, 2003 has multiple peaks. The flood on July 7, 2010 is a single-peak flood with extremely high maximum inflow water volume. The total durations of the two floods are 44 h and 145 h. The dispatching time intervals of the two floods are set to 3 h and 6 h respectively.

4.2. The preference model

The preference model is used to simulate the decision-making process of the decision maker at each scheduling time period. During the flood season, the water level of the reservoir has to be kept at the flood control limit level of 325 m, at the end of the operating horizon, with the aim of preparing for the next flood [17]. As a result, the candidate solution whose final upstream water level at the end of operating horizon is most close to 325 m will be the most preferred solution for the decision maker to adopt.

Fig. 4 illustrates the basic idea of the preference model, with which the most preferred solution can be identified from a set of candidate solutions provided by the DMO-RFC algorithm. It can be seen that the most preferred solution is the one

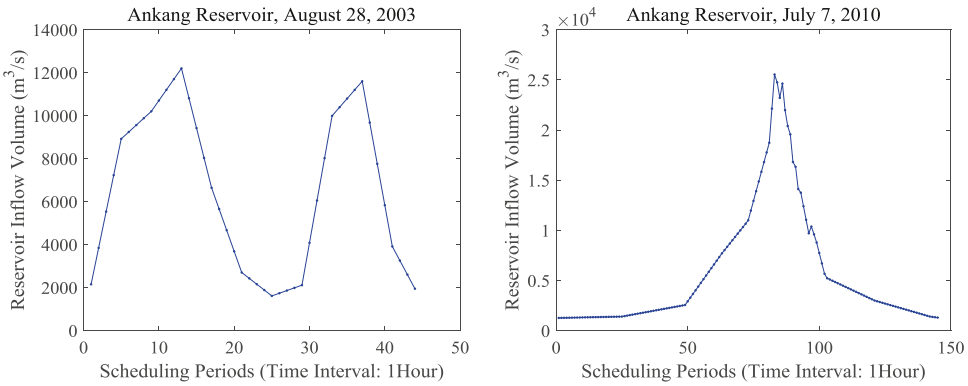

Fig. 3. Reservoir inflow of the two investigated floods.

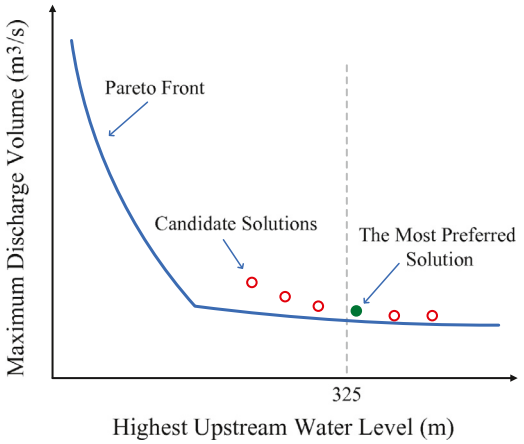

Fig. 4. The preference model for interactive decision-making.

whose highest upstream water level is the closest to 325 m. After determining the most preferred solution in the objective space based on the preference model, the corresponding preferred scheduling plan will be selected to put into practice. As shown in Fig. 1, the reservoir discharge volume at the next scheduling time period can be determined according to the selected scheduling plan.

4.3. The performance metric

Since the true Pareto front of each instantaneous multi-objective RFC problem is unavailable, the Hyper-volume metric [18] which is free from the true Pareto front is employed to evaluate the performance of the compared algorithms. Given a reference point R and an approximation set P obtained by a multi-objective optimization algorithm, the hyper-volume metric value is a measure of the region which is simultaneously dominated by P and bounded above by R. It can be mathematically defined as follows:

$$\text{HyperVolume}(P, R) = \text{Volume}\bigcup_{F\in P}\{x|F \prec x \prec R\} \tag{3}$$

In Eq. (3), F denotes a non-dominated solution in the Pareto approximation set of P. The reference point R is the user-defined reference point which is dominated by all valid candidate solutions in P. In the following experimental studies, the reference point is set to [400, 40000]. The hyper-volume metric is a comprehensive indicator of the quality of the obtained Pareto approximation set. A larger hyper-volume value indicates a better approximation of the true Pareto front.

4.4. Analysis on the dynamic multi-objective optimization model for RFC problem

By investigating the Pareto fronts of the sequence of instantaneous multi-objective RFC problems, this part of experiments is designed to perform some analysis on the change of the difficulty of the proposed dynamic multi-objective RFC model over time. Generally, it is impossible to give the exact mathematical expression of the true Pareto front of a multi-objective

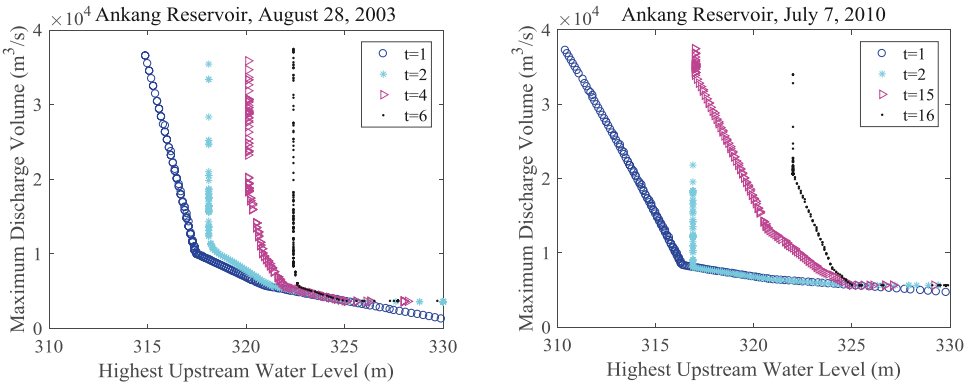

Fig. 5. Changes of the true Pareto fronts.

optimization model for real-world problems. Instead, it is a common and popular method in the field of evolutionary multi-objective optimization field to investigate the difficulty of the target problem by obtaining an approximation of the true Pareto front with satisfactory quality without considering the computational costs.

In order to achieve the most accurate approximation to the true Pareto front of each instantaneous problem, two implementations of the proposed DMO-RFC (RFC-NSGAII and RFC-MOEA/D which will be discussed in detail later) were run for enough iteration times of 100,000 to generate non-dominated solution sets with satisfactory quality for each instantaneous problem. Then, the non-dominated solutions were identified from the union set of the solutions obtained by the two DMO-RFC implementations, and used as the best approximation to the Pareto front of each instantaneous multi-objective RFC problem.

Fig. 5 illustrates the changes of the true Pareto fronts of the sequence of instantaneous multi-objective optimization problems in the proposed dynamic model for RFC Problem. It can be seen that the angles at knee region of the Pareto fronts become smaller and smaller over time. Since the sharp peak and low tail on the Pareto front raise big challenges to the multi-objective optimization algorithms [19], the difficulties of the instantaneous multi-objective optimization problems increase with time. To be specific, the sequence of instantaneous multi-objective optimization problems poses more and more challenges for the optimizers to achieve a satisfactory approximation set that covers the whole Pareto front of each instantaneous problem.

4.5. Effectiveness of the proposed algorithmic framework of DMO-RFC

In this part of experimental studies, two typical MOEAs, the NSGA-II algorithm [15] and the MOEA/D algorithm [16], are employed to generate two implementations of DMO-RFC, denoted as RFC-NSGAII and RFC-MOEA/D respectively. The NSGA-II algorithm is a Pareto dominance based algorithm and the MOEA/D algorithm is a decomposition based algorithm, they are the two most outstanding MOEAs with different types. By investigating these two implementations of DMO-RFC, the superiority of the proposed algorithmic framework for solving dynamic multi-objective RFC problems has been validated.

Due to the novelty of the proposed DMO model for RFC, no existing dynamic multi-objective optimization algorithm in literature can be directly employed to solve the new model. Instead, the algorithmic framework of DMO-RFC is developed in this work, following which any MOEA, like NSGA-II [15] and MOEA/D [16], can be employed as the population evolving algorithm at each scheduling time period.

With the aim of illustrating the superiority of the two developed change reaction strategies, the NSGA-II and MOEA/D algorithms are taken as the baseline algorithms in the experimental studies. It should be noted that, in the two baseline algorithms, the original NSGA-II and MOEA/D algorithms with random population initialization, simulated binary crossover and polynomial mutation [15,16] are employed as the population evolving algorithm at each scheduling time period, without using the two newly developed change reaction strategies.

In order to simulate the rolling reservoir inflow forecasting during floods, a random disturbance was added to each observed reservoir inflow to generate a simulated forecasting reservoir inflow with an average forecasting relative error of 10% (denoted as FRE=10%). RFC-NSGAII and RFC-MOEA/D were compared with the original NSGA-II and MOEA/D algorithms respectively. In which, the NSGA-II and MOEA/D algorithms mean that the two algorithms were employed to solve each instantaneous multi-objective RFC problem of the dynamic model in turn. The population sizes of RFC-NSGAII, RFC-MOEA/D and the compared algorithms were set to the same value of 200. The other parameter settings of NSGA-II and MOEA/D follow the suggestions by the authors in their papers [15] and [16].

4.5.1. Implementation 1: RFC-NSGAII

With the aim of illustrating the superiority of the two change reaction strategies in the algorithmic framework of DMO-RFC, the implementation of RFC-NSGAII was compared with the original NSGA-II which employs the random initialization

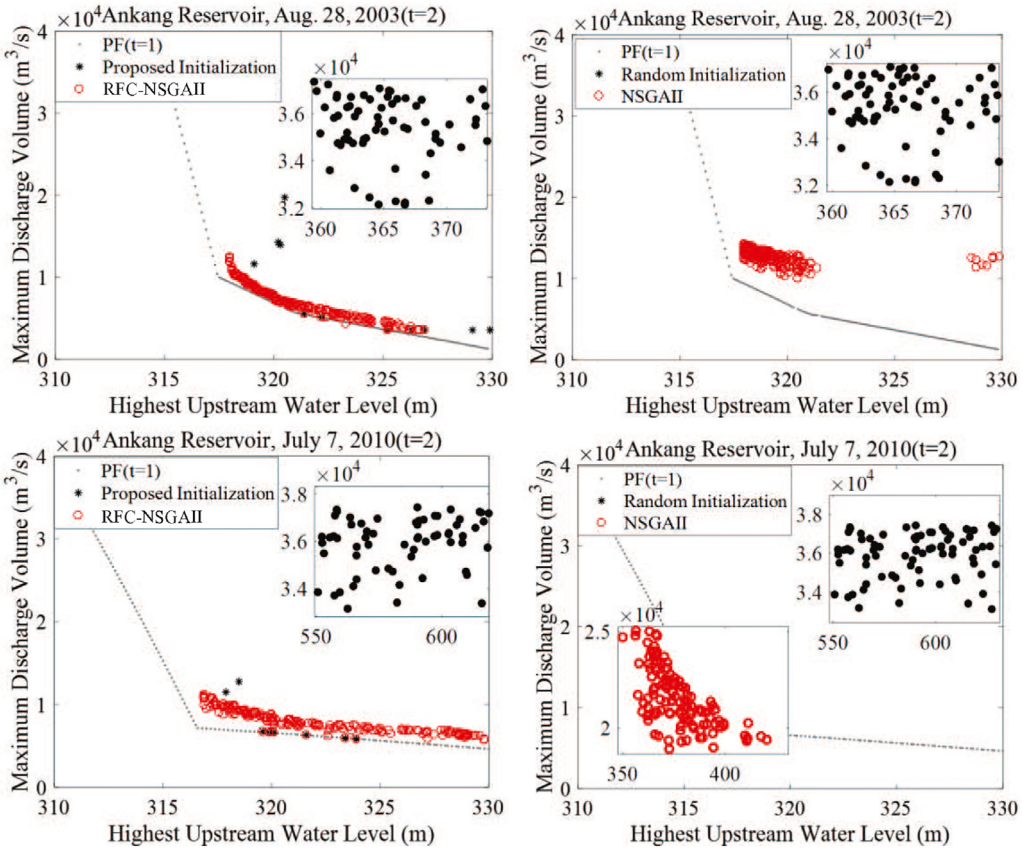

Fig. 6. RFC-NSGAII Vs. NSGA-II for the two investigated floods.

strategy and the simulated binary crossover [15] operator in the reproduction steps. Fig. 6 illustrates the distributions of non-dominated solutions obtained by RFC-NSGAII and NSGA-II on the two investigated floods. In these figures, both the initial population and the final evolved population obtained by the compared algorithms for the instantaneous multi-objective RFC problem at the tth scheduling time period are illustrated. Some of the points that locate out of the region of the main figure are plotted in the inset figure. The approximated true Pareto fronts with $t = 1$ (denoted as PF(t=1) in the figures) are taken as the base lines.

As shown in Fig. 6, the proposed initialization straggly generates 10% of the individuals by inheriting from the previous population, this part of individuals locates close to the target Pareto front, but fails to maintain satisfactory diversity especially at the late periods of the flood. While the rest 90% of the individuals were generated at random, which have a good diversity but locate far from the target Pareto front. Based on our observations, inherited individuals play important roles in accelerating the response speed of the algorithm to the changes of the model at the early periods of the flood. While the randomly generated individuals help to preserve diversity of the population and enhance the qualities of the obtained solutions at the early periods of the flood.

On the other hand, with the help of the DE-Operator, RFC-NSGAII obtained solution sets with much better convergence than that obtained by NSGA-II. For the flood on July 7, 2010 which is a big flood with an extremely high peak, the NSGA-II algorithm even failed to converge to the feasible region in the objective space. Therefore, the two change reaction strategies in DMO-RFC do help to enhance the performance of the NSGA-II algorithm on the dynamic multi-objective RFC problems. Following the proposed algorithmic framework of DMO-RFC, the implementation of RFC-NSGAII performs much better than the original NSGA-II algorithm both in convergence and diversity.

4.5.2. Implementation 2: RFC-MOEA/D

Similar experimental studies were conducted on another implementation of RFC-MOEA/D to validate the generalization of the proposed algorithmic framework for dynamic multi-objective RFC problems. Fig. 7 compares the performance of RFC-MOEA/D with the original MOEA/D algorithm on the two investigated floods. It can be seen that RFC-MOEA/D outperforms MEOA/D in term of convergence on all of the investigated floods, especially for the big flood on July 7, 2010.

The NSGA-II algorithm based on Pareto-dominance and the MOEA/D algorithm based on decomposition are the two most popular multi-objective evolutionary algorithms with different types. By validating the superiority of both RFC-NSGAII and

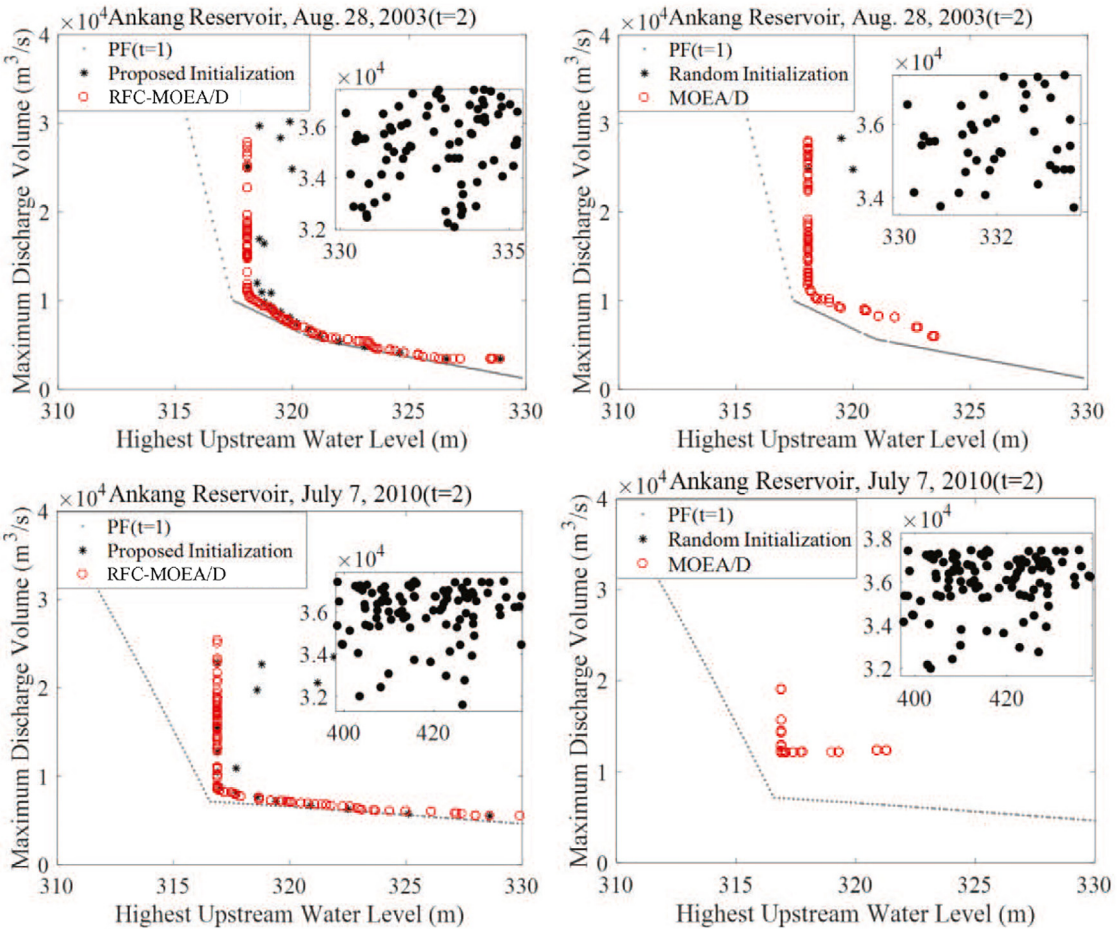

Fig. 7. RFC-MOEA/D Vs. MOEA/D for the two investigated floods.

RFC-MOEA/D, we can come to the conclusion that the proposed DMO-RFC is an effective and general algorithmic framework for solving the dynamic multi-objective RFC problems.

4.5.3. Response speed to the changes of the model

This part of experiments is designed to investigate the response speeds of RFC-NSGAII and RFC-MOEA/D to the changes of the model. Fig. 8 illustrates the superiority of the DMO-RFC implementations over their employed multi-objective evolutionary algorithms by comparing the changes of the average hyper-volume values during optimization and decision-making process. The experimental results in this figure are statistical values of 30 independent runs.

As shown in Fig. 8, the average hyper-volume values of RFC-NSGAII and RFC-MOEA/D decline less dramatically when changes happen, and rise up faster to higher values than NSGA-II and MOEA/D. Since a larger hyper-volume value indicates a better comprehensive performance, RFC-NSGAII and RFC-MOEA/D appear to be more responsive to the changes of the dynamic model. When comparing RFC-NSGAII with RFC-MOEA/D, the response speed of RFC-MOEA/D is faster than RFC-NSGAII, especially for the big flood on July 7, 2010. Meanwhile, MOEA/D converges to higher hyper-volume values than NSGA-II, which indicates that MOEA/D performs better than NSGA-II on the multi-objective RFC problems.

Tables 1 and 2 compare the performances of the algorithms on each instantaneous multi-objective RFC problem of the dynamic model, in term of the hyper-volume metric. The mean hyper-volume values and the standard deviations within parenthesis are compared. The Wilcoxon Rank-Sum test [20] with confidence level 0.95 has been applied to assess the statistical significance of the results.

In Tables 1 and 2, the symbols "+", "=" and "−" marked on the base line algorithms NSGA-II and MOEA/D respectively represent that the DMO-RFC implementations performances statistically better than, equivalent to and not as good as the base line algorithms. At the last line of each table, the comparison results are summarized by counting the times of Win/Tie/Loss (denoted as W/T/L) of each pair of compared algorithms.

As shown in Table 1, RFC-NSGAII outperforms NSGAII on 13 out of 14 comparisons, except for the first instantaneous multi-objective RFC problem, on which RFC-NSGAII performs as good as NSGAII. Comparing with MOEA/D, the RFC-MOEA/D

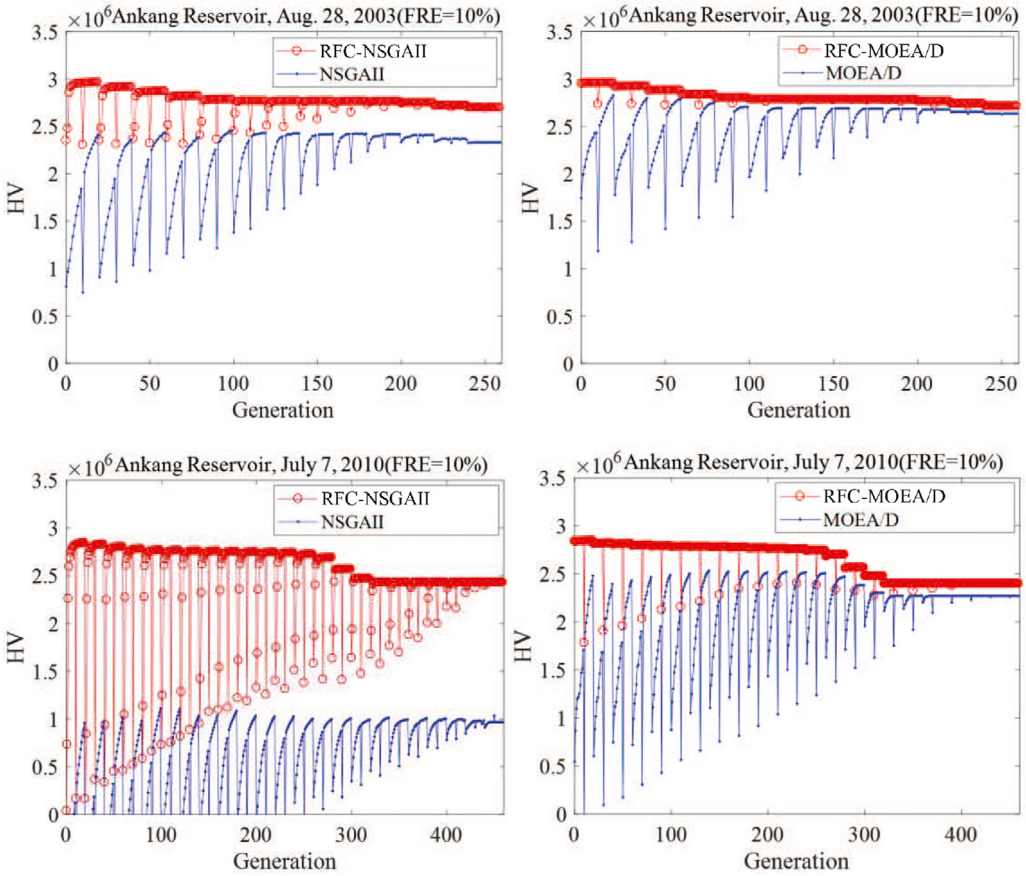

Fig. 8. Analysis on the response speed to the changes of the model.

Table 1
Performances on each instantaneous multi-objective RFC problem, based on the mean (standard deviation) of the hyper-volume values (Flood on Aug. 28, 2003).

t	Algorithms			
	RFC-NSGAII	NSGAII	RFC-MOEA/D	MOEA/D
1	3.283E+06(4.853E+02)	3.283E+06(4.853E+02)=	3.281E+06(2.275E+02)	3.281E+06(2.275E+02)=
3	**2.918E+06(2.313E+04)**	2.364E+06(1.510E+05)+	**2.925E+06(1.151E+04)**	2.799E+06(1.031E+05)+
5	**2.823E+06(2.521E+04)**	2.388E+06(1.774E+05)+	**2.838E+06(1.142E+04)**	2.751E+06(7.096E+04)+
7	**2.770E+06(2.455E+04)**	2.432E+06(2.307E+05)+	**2.788E+06(1.105E+04)**	2.694E+06(6.503E+04)+
9	**2.767E+06(2.429E+04)**	2.424E+06(2.329E+05)+	**2.785E+06(1.180E+04)**	2.691E+06(6.436E+04)+
11	**2.765E+06(2.417E+04)**	2.420E+06(2.327E+05)+	**2.783E+06(1.159E+04)**	2.687E+06(6.188E+04)+
13	**2.722E+06(2.464E+04)**	2.361E+06(2.719E+05)+	**2.740E+06(1.162E+04)**	2.655E+06(5.805E+04)+
14	**2.699E+06(2.537E+04)**	2.331E+06(2.796E+05)+	**2.717E+06(1.189E+04)**	2.635E+06(5.798E+04)+
W/T/L	13 / 1 / 0	0 / 1 /13	13 / 1 / 0	0 / 1 /13

algorithm wins 13 times and ties 1 time out of 14 comparisons. Similar conclusions on the other three investigated floods can be made based on the experimental results in Table 2. Thus, we can come to the conclusion that the DMO-RFC implementations outperform the employed multi-objective evolutionary algorithms significantly on the two investigated floods.

4.6. Robustness of DMO-RFC to the forecasting relative error

This part of experiments was designed to make a further investigation on the robustness of the proposed DMO-RFC framework to the forecasting relative error (FRE). Simulated forecasting reservoir inflows with average forecasting relative errors of 5% and 20% (respectively denoted as FRE=5% and FRE=20%) were generated to conduct the following experimental studies. Figs. 9 and 10 illustrate the changes of the average hyper-volume values of the two DMO-RFC implementations and the base line algorithms.

Table 2
Performances on each instantaneous multi-objective RFC problem, based on the mean (standard deviation) of the hyper-volume values (Flood on July 7, 2010).

t	Algorithms			
	RFC-NSGAII	NSGAII	RFC-MOEA/D	MOEA/D
1	3.245E+06(4.693E+02)	3.245E+06(4.693E+02)=	3.313E+06(1.181E+05)	3.313E+06(1.181E+05)=
3	**2.828E+06(2.553E+04)**	9.725E+05(3.541E+05)+	**2.819E+06(2.633E+04)**	2.395E+06(1.869E+05)+
5	**2.782E+06(2.979E+04)**	9.792E+05(4.341E+05)+	**2.799E+06(1.766E+04)**	2.465E+06(1.710E+05)+
7	**2.766E+06(2.755E+04)**	1.105E+06(6.284E+05)+	**2.786E+06(1.317E+04)**	2.503E+06(7.972E+04)+
9	**2.758E+06(2.363E+04)**	1.035E+06(6.401E+05)+	**2.781E+06(1.184E+04)**	2.522E+06(8.956E+04)+
11	**2.750E+06(2.140E+04)**	1.033E+06(7.569E+05)+	**2.770E+06(1.094E+04)**	2.514E+06(7.444E+04)+
13	**2.743E+06(1.992E+04)**	1.027E+06(7.680E+05)+	**2.760E+06(1.128E+04)**	2.516E+06(7.973E+04)+
15	**2.690E+06(1.780E+04)**	9.988E+05(7.665E+05)+	**2.702E+06(1.751E+04)**	2.471E+06(7.639E+04)+
17	**2.470E+06(2.867E+04)**	9.944E+05(7.222E+05)+	**2.477E+06(2.259E+04)**	2.303E+06(7.140E+04)+
19	**2.431E+06(2.901E+04)**	9.943E+05(7.119E+05)+	**2.397E+06(3.449E+04)**	2.272E+06(7.210E+04)+
21	**2.431E+06(2.894E+04)**	1.003E+06(7.052E+05)+	**2.397E+06(3.449E+04)**	2.272E+06(7.210E+04)+
23	**2.430E+06(2.903E+04)**	9.842E+05(6.914E+05)+	**2.397E+06(3.449E+04)**	2.272E+06(7.210E+04)+
24	**2.430E+06(2.877E+04)**	9.677E+05(6.780E+05)+	**2.397E+06(3.471E+04)**	2.272E+06(7.210E+04)+
W/T/L	23 / 1 / 0	0 / 1 / 23	23 / 1 / 0	0 / 1 / 23

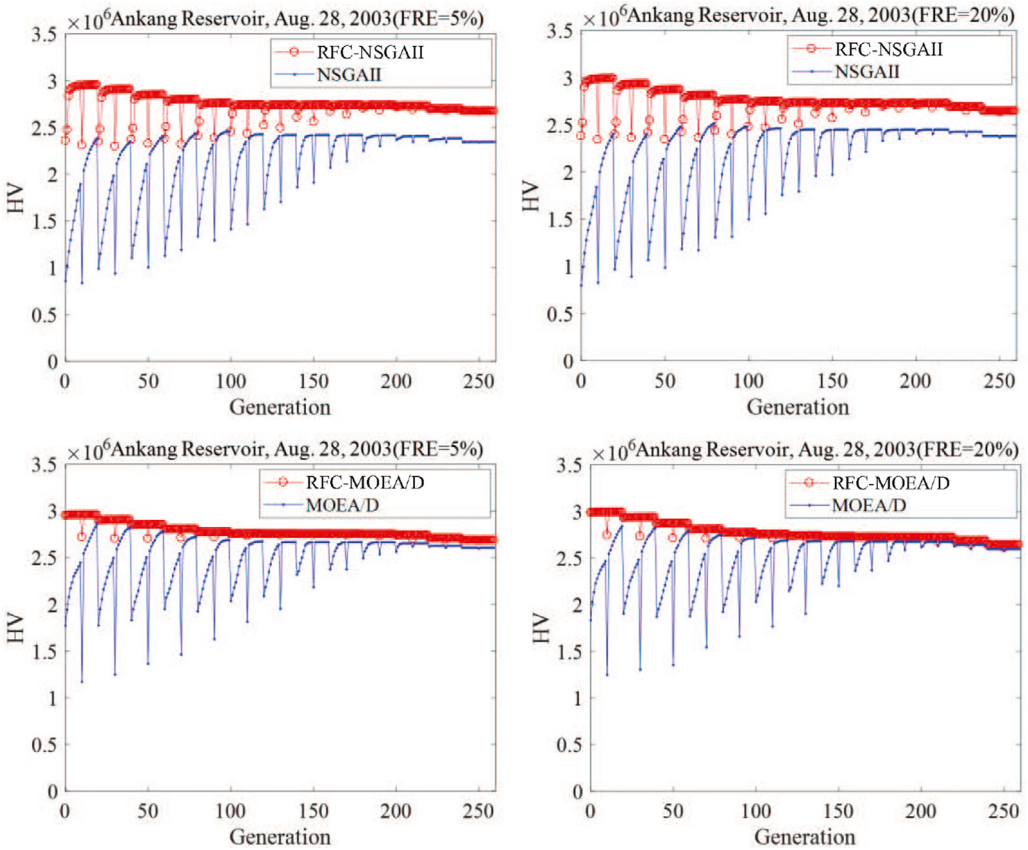

Fig. 9. Robustness to the forecasting relative error (Flood on Aug. 28, 2003).

As shown in Figs. 9 and 10, the forecasting relative error has no significant effect on the response speeds of both the DMO-RFC implementations and the base line algorithms to the changes. But it will affect the quality of the solution sets obtained by the compared algorithm.

In addition, the hyper-volume curves of DMO-RFC implementations and the base line algorithms converge to lower values when the average forecasting relative error is large, which indicates the fact that a large forecasting error will degenerate the performance of the multi-objective optimizer, especially for the instantaneous multi-objective RFC problems at the late periods of the flood.

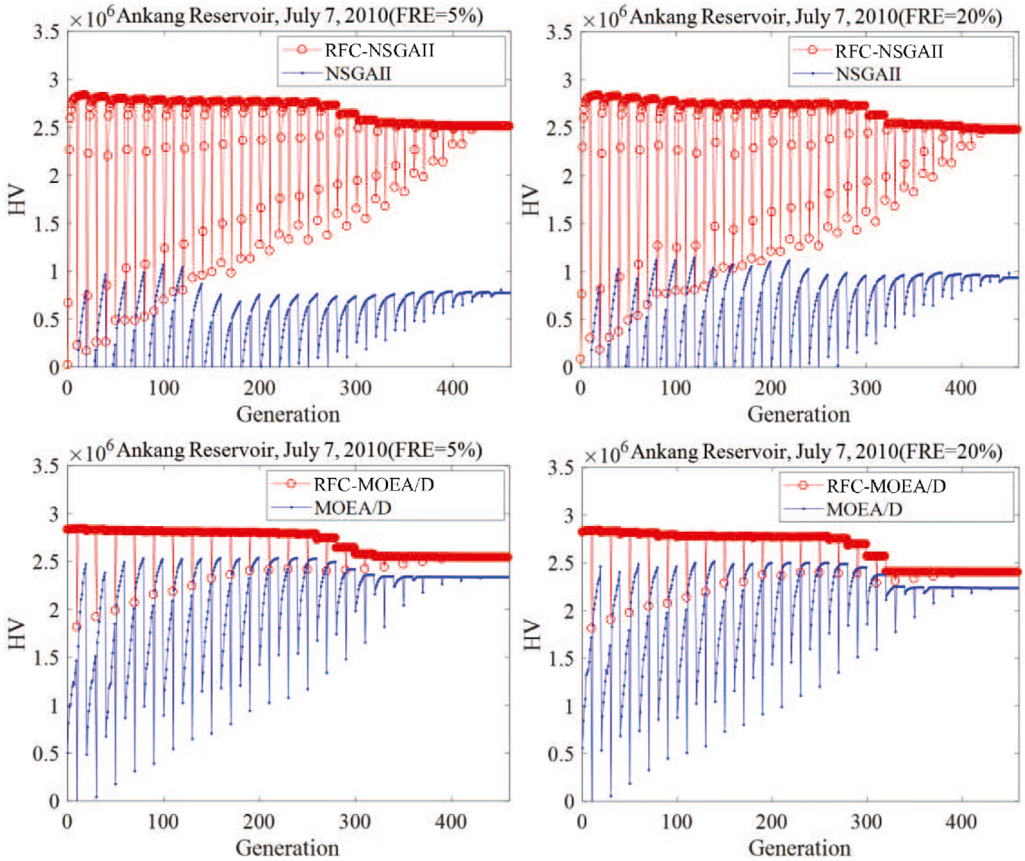

Fig. 10. Robustness to the forecasting relative error (Flood on July 7, 2010).

Table 3
Reservoir operation policies in use at the Ankang reservoir.

Policy no.	Inflow Q_{in} (m^3/s)	Water level Z (m)	Discharge Q_{out} (m^3/s)
1	$12000 < Q_{in} \leq 15100$	$Z \leq 326$	$Q_{out} = 12000$
2	$12000 < Q_{in} \leq 15100$	$Z > 326$	$Q_{out} = Q_{in}$
3	$15100 < Q_{in} \leq 17000$	$Z > 326$	$Q_{out} = Q_{in}$
4	$17000 < Q_{in} \leq 21500$	$326 < Z \leq 328$	$Q_{out} = 17000$
5	$17000 < Q_{in} \leq 21500$	$Z > 328$	$Q_{out} = Q_{in}$
6	$21500 < Q_{in} \leq 24200$	$Z > 328$	$Q_{out} = Q_{in}$
7	$Q_{in} > 24200$	–	Free discharge

4.7. Superiority over operation policies in use at the Ankang reservoir

Based on the flood control standard at the Ankang reservoir, reservoir operation policies have been developed by hydrologists to provide a guidance for real-time reservoir flood control. Table 3 shows the details of the operation policies in use at the Ankang reservoir.

It can be seen that Table 3 provides a rough reservoir operation rule in which the discharge volume Q_{out} equals to the water inflow volume Q_{in} in most cases. If a 5-year flood occurs ($12000 < Q_{in} \leq 15100$), the reservoir controls the flood and discharges at a rate of $12{,}000\,m^3/s$. If a 20-year flood occurs ($17000 < Q_{in} \leq 21500$), the discharge rate cannot exceed $17{,}000\,m^3/s$.

To illustrate the superiority of the DMO-RFC implementations, Table 4 compares the reservoir operation schemes determined by the proposed algorithm and the reservoir operation policies in use at the Ankang reservoir. As shown in Table 4, the two DMO-RFC implementations RFC-NSGAII and RFC-MOEA/D can provide more refined reservoir operation schemes with lower maximum discharge volumes and highest upstream water levels, which indicates the fact that the DMO-RFC implementations perform significantly better than the reservoir operation policies in terms of both the flood peak reduction and the upstream side safety.

Table 4
Reservoir operation schemes determined by the DMO-RFC implementations and the reservoir operation policies in use (Q_{MaxIn} represents the maximum reservoir inflow, Q_{Max} denotes the maximum discharge volume, Z_{Max} means the highest upstream water level, Z_{End} is the water level at the end of the scheduling periods).

Floods	Q_{MaxIn}	RFC-NSGAII			RFC-MOEA/D			Operation policies		
(Year)	(m^2/s)	Q_{Max} (m^2/s)	Z_{Max} (m)	Z_{End} (m)	Q_{Max} (m^2/s)	Z_{Max} (m)	Z_{End} (m)	Q_{Max} (m^2/s)	Z_{Max} (m)	Z_{End} (m)
Oct. 12, 2000	17730	9973.35	325.4	315.8	7817.8	324.96	321.349	17000	327.4	327.4
Aug. 28, 2003	12200	8275.3	324.9	324.9	3558.5	325.07	325.03	11600	326.3	326.3
Oct. 01,2005	21000	13416	325.6	321.1	11951	325.02	324.5	18000	328.1	328.1
July 07, 2010	25537	6394.17	325	322.1	5958.2	324.95	322.33	25537	326.9	326.9

5. Conclusions and future works

Reservoir flood control operation (RFC) is complex multi-objective optimization problem that involves multiple conflicting objectives and a dynamic decisions-making environment. Although techniques of multi-objective optimization and uncertainty handling in reservoir flood control have been intensively studied in recent years, no work has been done yet on developing and investigating dynamic multi-objective optimization models for this problem.

In this paper, a dynamic multi-objective optimization model with interactivity and uncertainty was developed at first. Then, a dynamic multi-objective algorithmic framework with two newly designed change reaction strategies, denoted as DMO-RFC, was proposed. The proposed dynamic model considers the uncertainty of the reservoir forecasting error, and works interactively with the decision maker. Following the DMO-RFC algorithmic framework, any evolutionary multi-objective optimization algorithm can be converted into a dynamic optimizer for solving the proposed optimization model. Two DMO-RFC implementations combining with the two most popular multi-objective optimization algorithms with different types, i.e. the NSGA-II and the MOEA/D algorithms, were investigated. Two typical floods of Ankang reservoir were used as the study cases. According to the experimental results, we can come to the following conclusions.

1. The challenge of the instantaneous multi-objective RFC problem at each scheduling time period in the proposed dynamic multi-objective optimization model increases with time.
2. The two newly designed change reaction strategies in DMO-RFC can significantly improve the performances of the employed multi-objective optimizers on the dynamic multi-objective RFC problems, in terms of both convergence and diversity.
3. The good performances of the two implementations of RFC-NSGAII and RFC-MOEA/D indicate the fact that the proposed DMO-RFC is an effective and general algorithmic framework for solving the proposed model.
4. The response speed of DMO-RFC is not significantly influenced by the reservoir inflow forecasting error, it is a robust algorithmic framework.

Further research efforts may focus on providing the decision-maker with more convenient interactive models and developing more powerful change reaction mechanisms in DMO-RFC which makes a good balance between the response speed and the qualities of the obtained solutions.

Acknowledgments

This work was supported by the National Natural Science Foundation of China under Grant nos. 51679186 and 61772392, the National Key R&D Program of China under Grant no. 2016YFC0401409.

References

[1] S. Hajkowicz, K. Collins, A review of multiple criteria analysis for water resource planning and management, Water Resour. Manag. 21 (9) (2007) 1553–1566.
[2] J. Chang, X. Meng, Z. Wang, X. Wang, Q. Huang, Optimized cascade reservoir operation considering ice flood control and power generation, J. Hydrol. 519, Part A (2014) 1042–1051.
[3] F. Wang, O. Saavedra Valeriano, X. Sun, Near real-time optimization of multi-reservoir during flood season in the fengman basin of china, Water Resour. Manag. 27 (12) (2013) 4315–4335.
[4] H. Qin, J. Zhou, Y. Lu, Y. Li, Y. Zhang, Multi-objective cultured differential evolution for generating optimal trade-offs in reservoir flood control operation, Water Resour. Manag. 24 (11) (2010) 2611–2632.
[5] J. Luo, Y. Qi, J. Xie, X. Zhang, A hybrid multi-objective pso-eda algorithm for reservoir flood control operation, Appl. Soft Comput. 34 (2015) 526–538.
[6] C. Chaleeraktrakoon, Y. Chinsomboon, Dynamic rule curves for flood control of a multipurpose dam, J. Hydro Environ. Res. 9 (1) (2015) 133–144.
[7] M. Feng, P. Liu, S. Guo, Z. Gui, X. Zhang, W. Zhang, L. Xiong, Identifying changing patterns of reservoir operating rules under various inflow alteration scenarios, Advan. Water Resour. 104 (2017) 23–36.
[8] F.N.-F. Chou, C.-W. Wu, Stage-wise optimizing operating rules for flood control in a multi-purpose reservoir, J. Hydrol. 521 (2015) 245–260.
[9] S. Jiang, S. Yang, Evolutionary dynamic multiobjective optimization: benchmarks and algorithm comparisons, IEEE Trans. Cybern. 47 (1) (2017) 198–211.
[10] Z. Zhang, Multiobjective optimization immune algorithm in dynamic environments and its application to greenhouse control, Appl. Soft Comput. 8 (2) (2008) 959–971.
[11] M. Jiang, Z. Huang, L. Qiu, W. Huang, G.G. Yen, Transfer learning based dynamic multiobjective optimization algorithms, IEEE Trans. Evol. Comput. 22 (4) (2018) 501–514.

[12] S.B. Gee, K.C. Tan, H.A. Abbass, A benchmark test suite for dynamic evolutionary multiobjective optimization, IEEE Trans. Cybern. 47 (2) (2017) 461–472.
[13] J. Ding, C. Yang, Q. Xiao, T. Chai, Y. Jin, Dynamic evolutionary multiobjective optimization for raw ore allocation in mineral processing, IEEE Trans. Emerg. Top. Comput. Intell. 3 (1) (2019) 36–48.
[14] Y. Qi, Z. Hou, M. Yin, H. Sun, J. Huang, An immune multi-objective optimization algorithm with differential evolution inspired recombination, Appl. Soft Comput. 29 (2015) 395–410.
[15] K. Deb, A. Pratap, S. Agarwal, T. Meyarivan, A fast and elitist multiobjective genetic algorithm: NSGA-II, IEEE Trans. Evol. Comput. 6 (2) (2002) 182–197.
[16] Q. Zhang, H. Li, MOEA/D: a multiobjective evolutionary algorithm based on decomposition, IEEE Trans. Evol. Comput. 11 (6) (2007) 712–731.
[17] Y. Qi, J. Yu, X. Li, Y. Wei, Q. Miao, Reservoir flood control operation using multi-objective evolutionary algorithm with decomposition and preferences, Appl. Soft Comput. 50 (2017) 21–33.
[18] E. Zitzler, L. Thiele, Multiobjective evolutionary algorithms: a comparative case study and the strength Pareto approach, IEEE Trans. Evol. Comput. 3 (4) (1999) 257–271.
[19] Y. Qi, X. Ma, F. Liu, L. Jiao, J. Sun, J. Wu, MOEA/D with adaptive weight adjustment, Evol. Comput. 22 (2) (2014) 231–264.
[20] F. Wilcoxon, Individual comparisons by ranking methods, Biom. Bull. 1 (6) (1945) 80–83.